Organic & Biomolecular Chemistry

PAPER

Computational study of radicals derived from hydroxyurea and its methylated analogues†

Ivana Vinković Vrček,[a] Davor Šakić,[b] Valerije Vrček,*[b] Hendrik Zipse[c] and Mladen Biruš[b]

Structural and electronic properties and chemical fate of free radicals generated from hydroxyurea (HU) and its methylated analogues *N*-methylhydroxyurea (NMHU) and *O*-methylhydroxyurea (OMHU) are of utmost importance for their biological and pharmacological effects. In this work the *cis/trans* conformational processes, tautomerizations, and intramolecular hydrogen and methyl migrations in hydroxyurea-derived radicals have been considered. Potential energy profiles for these reactions have been calculated using two DFT functionals (BP86 and B3LYP) and two composite models (G3(MP2)RAD and G3B3). Solvation effects have been included both implicitly (CPCM) and explicitly. It has been shown that calculated energy barriers for free radical rearrangements are significantly reduced when a single water molecule is included in calculations. In the case of HU-derived open-shell species, a number of oxygen-, nitrogen-, and carbon-centered radicals have been located, but only the *O*-centered radicals (*e1* and *z1*) fit to experimental isomeric hyperfine coupling constants (hfccs) from EPR spectra. The reduction of NMHU and OMHU produces *O*-centered and *N*-centered radicals, respectively, with the former being more stable by *ca.* 60 kJ mol⁻¹. The NMHU-derived radical *e4* undergoes rearrangements, which can result in formation of several conceivable products. The calculated hfccs have been successfully used to interpret the experimental EPR spectra of the most probable rearranged product **10**. Reduction potentials of hydroxyureas, radical stabilization energy (RSE) and bond disocciation energy (BDE) values have been calculated to compare stabilities and reactivities of different subclasses of free radicals. It has been concluded, in agreement with experiment, that reductions of biologically relevant tyrosyl radicals by HU and NMHU are thermochemically favorable processes, and that the order of reactivity of hydroxyureas follows the experimentally observed trend NMHU > HU > OMHU.

Introduction

Hydroxyurea (HU) or hydroxycarbamide has been of scientific and clinical interest for more than 100 years.[1] HU is structurally related to hydroxamic acids (Chart 1), known as metal chelators and microbial siderophores characterised by diverse biological activities such as antibacterial, antifungal, antitumor and anti-inflammatory activities.[2–4] HU acts as a source of nitric oxide (NO), which plays an important role in the maintenance of normal blood pressure and flow.[5] Nowadays, it is used to treat leukemia and other malignances, sickle-cell anemia, HIV infection, thrombocythemia, psoriasis and polycythemia vera.[6]

[a] Institute for Medical Research and Occupational Health, Ksaverska cesta 2, 10 001, Zagreb, Croatia. E-mail: valerije@pharma.hr; Fax: +385 1 4856201; Tel: +385 1 6394441

[b] University of Zagreb, Faculty of Pharmacy and Biochemistry, A. Kovačića 1, HR-10000, Zagreb, Croatia

[c] Department of Chemistry, LMU München, Butenandstr. 13, D-81377, München, Germany
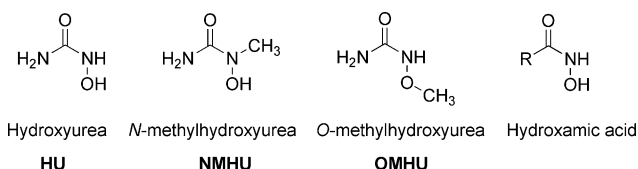
Chart 1 Hydroxyurea, its methylated derivatives, and general structure of hydroxamic acid.

The interest in HU is particularly caused by its specific target ribonucleotide reductase (RNR), the enzyme responsible for the synthesis of deoxyribonucelotides from ribonucleotides.[7,8] Several lines of evidence have indicated that RNR is the primary, if not only, cellular target of HU.[9–12] The mechanism by which HU causes cell death, however, has remained obscure.[13,14]

The pharmacological effects of HU and its derivatives has been attributed not only to enzyme inhibition or metal chelation, but also to its ability to serve as nitroxyl (HNO/NO⁻) and nitric oxide donors.[15] It has been reported that HNO and NO are formed upon oxidation of HU chemically,[16] enzymatically,[5,17] or by the combination of heme proteins and H_2O_2.[18] Nitric oxide

formation from hydroxyurea requires a three-electron oxidation, which may proceed either through the nitroxide radical or a *C*-nitroso intermediate.[5,19] The remainder of the HU molecule may decompose into formamide or carbon dioxide and ammonia, depending on the conditions and type of oxidant employed.[20] However, the mechanism for the formation of reactive nitrogen species from HU is not clear and requires further elucidation.

Recently, King and co-workers demonstrated experimentally that some derivatives of hydroxyurea can generate nitroxide radicals more rapidly than hydroxyurea.[21] Furthermore, Rohrman and Mazziotti showed that the effectiveness of different hydroxyurea derivatives to generate nitroxide radicals depends on relative O–H bond dissociation energies.[22] Thus, electrochemical processes brought on by transformations of HU in a cell may also be triggered by structural requirements. The tuning of the stability of the nitroxide radicals constitutes an effective method to increase the efficiency of the hydroxyurea-based drugs and quantum mechanical calculations can act as an effective tool for that challenge. The intermediacy of carbon- or heteroatom-centered radicals is of special importance for the biological activity of hydroxyurea. For example, mechanisms of inhibition of ribonucleotide reductase,[23–25] ascorbate peroxidase,[26] or oxygenic photosystem II[27] are closely related to the nature of the respective free radicals. In general, nitrogen-centered radicals are more electron-deficient species as compared to the corresponding carbon-centered analogs, while the substituent effects on their stabilities are similar to those for oxygen-centered radicals.[28,29] In this work, we have applied several computational models, which provide a useful approach in giving insight into the mechanism

underlying the formation and rearrangements of hydroxyurea-derived radicals.

Furthermore, we have recently shown that oxidation of HU, *N*-methylhydroxyurea (NMHU) and *O*-methylhydroxyurea (OMHU) with ferricyanide in water does not correlate with the basicity of hydroxyureas, but could rather depend on the localization of the electron spin density within the particular free radical.[30] The HU free radical was characterized by EPR spectroscopy quite some time ago, and we recently characterized free radicals of NMHU by the same method,[31] but have failed to characterize the free radical of OMHU.[30] Therefore, in this work, we have applied several computational models, which reasonably well confirm the spectroscopic results on HU and NMHU, hence providing a useful approach, giving insight both into the structure of the free radicals derived from all three hydroxyureas, as well as the mechanism underlying their formation and subsequent rearrangements.

Results and discussion

Hydroxyurea-derived radicals

The chemical fate of free radicals formed *via* oxidation of hydroxyurea (HU) or aminoformohydroxamic acid is not clear. Several possible pathways have been suggested for its decomposition. EPR studies show the formation of the nitroxide radical (*e1/z1*, Scheme 1), which has been proposed to decompose to NO, during the reaction of HU with hemoglobin or metal ion oxidants. However, the detailed molecular mechanism describing the actions of HU
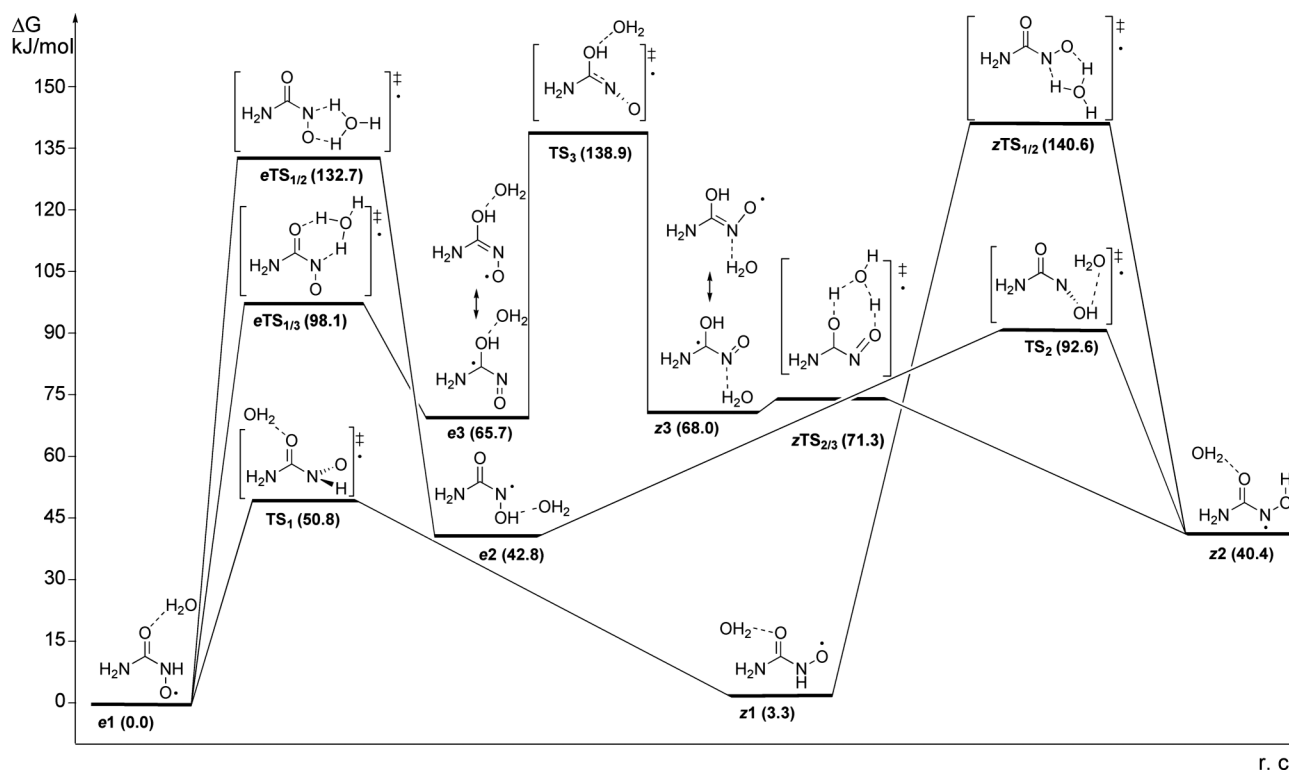
Scheme 1 Schematic potential energy profile (G3B3 + ΔG_{solv}) for isomerization and rearrangement processes in *O*- (**1**), *N*- (**2**), and *C*-centered (**3**) hydroxyurea radicals. Only the most stable water-complexed structure is presented for each species. The energy of water-complexed *O*-radical *e1* is set to zero.

remains to be established. In the present study, the rearrangements of the parent nitroxide radical $e1/z1$ have been investigated computationally, including *cis/trans* isomerization and intramolecular hydrogen migration as elementary reaction steps. In addition to *O*-centered radical $e1/z1$, both *N*- ($e2/z2$) and *C*-centered ($e3/z3$) radicals have been located on the corresponding potential energy surface (Scheme 1). According to earlier experimental studies the oxygen-centered radical $e1/z1$ is formed during one-electron oxidation of hydroxyurea. It has been observed by EPR spectroscopy, but no detailed information on its geometry is available. In the present study, several computational techniques have been employed in order to characterize structural and electronic properties of this radical and its rearranged products.

Two different forms of *O*-centered radical have been located, $e1$ and $z1$, in which carbonyl and hydroxyl oxygen atoms are in *trans* or *cis* relative orientation, respectively (Scheme 1, Fig. 1). In the gas phase (no explicit water included) the isomer $e1$ is lower in energy (more stable by 20–40 kJ mol⁻¹, depending on the theoretical model, see ESI†) and has a planar symmetrical structure (C_s point group),[32] while the symmetrical structure of $z1$ corresponds to a first-order saddle point (NImag = 1). The minimum structure of $z1$ deviates from planarity and is slightly pyramidal at the NH_2 nitrogen atom.[33] In order to consider specific solvent interactions

with the free radical intermediates, a discrete water molecule is included in each examined species (see below). We have shown earlier that a single water molecule is also sufficient to properly describe water-assisted radical rearrangements.[34] When both implicit (CPCM) and explicit solvent effects are included (Table 1), radicals $e1$ and $z1$ become similar in energy (*i.e.* the former being more stable by 3.3 kJ mol⁻¹). In both isomers the spin density is delocalized over the hydroxamate moiety as illustrated by the singly occupied molecular orbitals (SOMOs) that mostly include O and N atoms with some delocalization over the carbonyl oxygen (Fig. 1). The experimental EPR signal of the free radical derived from hydroxyurea consists of six resonance lines characteristic of the aminocarbonylaminoxyl radical H_2N–CO–$NHO^{\bullet}$.[35,37] It is brought about by coupling of the unpaired electron with the ¹⁴N nucleus (a_N = 8.0 gauss), giving rise to triplet resonance lines, while further splitting into doublets is caused by proton coupling (a_H = 12.0 gauss). The capability of the B3LYP functional, combined with the EPR-III basis set,[37] to reproduce the experimental isotropic hyperfine coupling constants (hfccs) has been reported for a large set of organic radicals.[38]

We have applied the computational procedure of Hermosilla *et al.*[38] to test if the calculated hfcc values can be used to differentiate between $e1$ and $z1$ isomers. Interestingly, calculations for the two isomers have produced hfccs results which both agree with experimental data (Table 2). In order to confirm that the isotropic hfcc is related to the spin density at the nucleus, we have calculated the spin distribution in $e1$ and $z1$. The calculated Mulliken values indicate that the unpaired electron in $e1$ and $z1$ is mostly localized at O and N atoms (Fig. 1). It comes out that similar atomic spin densities in $e1$ and $z1$ correlate well with calculated hfccs in these two radicals. On the basis of the small energy difference between the *trans* and *cis* isomers (ΔG ~ 3 kJ mol⁻¹), it is estimated that both $e1$ and $z1$ contribute to the averaged spectroscopic properties of the hydroxyurea radical.

Three different types of rearrangements of hydroxyurea radicals have been considered: the isomerization of the *cis* and *trans* forms, the hydrogen migration between N and O atoms of the hydroxamate moiety, and the tautomerization equilibrium in which amidic (hydroxamic) and iminolic (hydroximic) form coexist (Scheme 1). The transition state structure TS_1 for interconverting
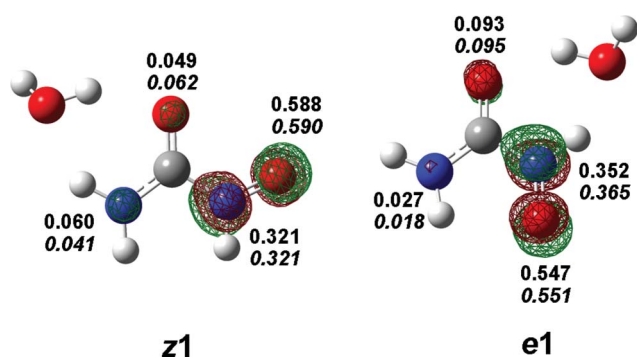

Fig. 1 UBP86/6-311++G(d,p) calculated SOMOs and spin distributions (Mulliken values) in water-complexed hydroxyurea radicals $e1$ and $z1$. Spin density values for gas-phase geometries (no explicit water is included) are in italics.

Table 1 Relative energies (ΔG in kJ mol⁻¹, at 298.15 K) for structures involved in isomerization and rearrangement reactions of hydroxyurea-derived radicals

Name[a]	UBP86[b]	UB3LYP[b]	G3(MP2)RAD	G3B3	ΔG_{solv}[c]	G3B3 + ΔG_{solv}
$e1$	0.0	0.0	0.0	0.0	−54.2	0.0
$z1$	33.6	30.4	34.5	34.5	−85.4	3.3
$e2$	54.2	55.9	52.3	50.2	−61.6	42.8
$z2$	34.2	40.1	35.6	36.5	−50.3	40.4
$e3$	59.2	69.6	65.4	67.4	−55.9	65.7
$z3$	53.8	76.8	75.7	76.8	−63.0	68.0
TS_1	62.9	62.2	63.2	64.8	−68.2	50.8
TS_2	84.4	87.7	75.5	104.3	−65.9	92.6
TS_3	164.6	156.7	152.9	156.6	−71.9	138.9
$eTS_{1/2}$	111.9	130.6	133.2	132.3	−53.8	132.7
$zTS_{1/2}$	130.6	149.3	150.6	151.6	−65.2	140.6
$eTS_{1/3}$	75.2	90.1	90.0	92.8	−48.9	98.1
$zTS_{2/3}$	60.7	89.4	89.7	90.1	−73.0	71.3

[a] The most stable conformer considered. [b] 6-311++G(d,p) basis set employed. [c] Solvation energies calculated with CPCM/UAKS/UB3LYP/6-311+G(d,p) method in the model solvent (water) of ε = 78.4.

Table 2 UB3LYP//UB3LYP/6-31G(d) calculated hfccs (a_{iso} in gauss)[a] for water-complexed hydroxyurea-derived radicals

	Isotropic hfccs	
Radical[b]	a_N	a_H
e1	8.0 (8.1)[c]	12.4 (12.4)
z1	7.1 (7.3)	11.9 (12.0)
e2	14.8 (15.7)	5.9 (5.6)
z2	13.8 (14.1)	6.9 (6.9)
e3	4.9 (3.7)	1.5 (1.5)
z3	6.6 (5.2)	1.4 (1.4)
Exp.[d]	*8.0*	*12.0*

[a] The EPR-III basis set employed for C, H, and O atoms, and 6-31G(d) basis set for N atoms. [b] The most stable conformer considered. [c] Calculated hfccs for gas-phase geometries (no explicit water included) in parentheses. [d] From ref. 34.

e1 and **z1** is characterized by one imaginary frequency ($180i$ cm^{-1}), which corresponds to rotation around the (O)C–N(O) bond. The relatively high rotational energy barrier of 51.1 kJ mol^{-1} is due to the loss of its partial double bond character.[39,40] In addition, transition state structures **eTS$_{1/2}$** and **zTS$_{1/2}$**, which connect *O*-centered radicals **e1** and **z1** with the corresponding *N*-centered radicals **e2** and **z2**, respectively, have been located on the potential energy surface. This hydrogen migration is a water-assisted process, for which the inclusion of a discrete water molecule in the corresponding transition state structure is mandatory. If one explicit water molecule is well placed to facilitate hydrogen migration, the calculated barrier for the 1,2-[N↔O]-H shift is significantly lower in energy than the corresponding hydrogen shift in the gas phase. This is in agreement with earlier studies, which have reported the participation of water in hydrogen migrations in free radicals.[41] Three different pathways of water-catalyzed mechanisms (see ESI†) have been considered, but only the most feasible processes, in which the water molecule is directly involved in forming five-membered ring transition states **eTS$_{1/2}$** and **zTS$_{1/2}$**, are presented in the Scheme 1. The calculated energy barriers for hydrogen migrations *via* **eTS$_{1/2}$** and **zTS$_{1/2}$** are 132.7 and 140.6 kJ mol^{-1}, respectively, which suggests that these processes are kinetically unfavorable. The resulting *N*-centered radicals **e2** and **z2** are less stable than the *O*-radicals, **e1** and **z1** (Scheme 1). In contrast to *O*-radicals, the calculated hfccs for *N*-radicals deviate strongly from the experimental data (Table 2). All these data support the proposal from experimental studies in which only *O*-centered radicals have been considered as the relevant oxidation products of hydroxyurea.

The least stable radicals derived from hydroxyurea are formally designated as carbon-centered radicals **e3** and **z3**, which are presented in Scheme 1 with two resonance structures each.[42] They exist in conformational equilibrium, but the transition state structure **TS$_3$** which connects them is very high in energy (Scheme 1). The *C*-radicals **e3** and **z3** are hydroximic tautomers of the *O*-radical **e1** and *N*-radical **z2**, respectively. The transition state structure **eTS$_{1/3}$** connecting **e1** and **e3** is characterized by a six-membered ring, in which one water molecule assists the proton transfer process and is located 98.1 kJ mol^{-1} above the global minimum **z1**. Therefore, the tautomerization of *O*-radical **e1** *via* **eTS$_{1/3}$** is a more feasible rearrangement (the calculated rate constants k = 4×10^{-5} s^{-1}) than the hydrogen migration *via* **eTS$_{1/2}$**

(k < 3.5×10^{-11} s^{-1}).[43] Similarly to the case of *N*-radicals, a large discrepancy between experimental and calculated isotropic hfcc values can be observed for the *C*-radicals (Table 2). In conclusion, only the oxygen-centered radicals **e1** and **z1** are relevant open-shell intermediates derived through hydrogen abstraction from hydroxyurea. Both nitrogen- and carbon-centered radicals are significantly higher in energy and display spectroscopic characteristics in significant disagreement with experiment.

N-Methylhydroxyurea-derived radicals

N-methylhydroxyurea (NMHU) and *O*-methylhydroxyurea (OMHU) are important kinetic and mechanistic probes for the reaction of hydroxyurea and hydroxamic acids with hemoglobin. The OMHU is unreactive towards this metalloprotein, and the *N*-methylated derivative of HU reacts with both oxy- and methemoglobin, but the overall reaction mechanism is somewhat different.[21,44] Unlike HU, which is a source of nitric oxide (NO), NMHU and its open shell forms cannot transfer NO to hemoglobin as the NO transfer requires an unsubstituted acylhydroxylamine group. In addition, the oxidations of NMHU and OMHU with metal ions are characterized by a peculiar behavior (see below) of the observed intermediates,[30,31] which warrants a comparative study of open-shell intermediates derived from HU, NMHU, and OMHU.

Contrary to the case of hydroxyurea radical, where O-, *N*- and *C*-radicals interconvert through proton migration reactions (Scheme 1), comparable rearrangement reactions are not possible in the *O*-centered *N*-methylhydroxyurea radical **e4**. For example, the calculated energy barrier for 1,2-[N↔O]-methyl shift, which transforms the *O*-centered *N*-methylhydroxyurea radical (**e4**) to the *N*-centered methoxyurea radical (**e5**), is extremely high (Scheme 2). The transition state **eTS$_{4/5}$** is calculated >300 kJ mol^{-1} higher in energy than **e4** making the rearrangement process **e4** → **e5** quite unlikely. The analogous transition state **zTS$_{4/5}$** which equilibrates radicals **z4** and **z5** is even higher in energy (Table 3).

A more favorable three-step process, which can rearrange **e4** to **z5** through radical intermediates **e8** and **z8**, is also conceivable (Scheme 3). As a first step this involves the formal 1,3-[N↔O]-methyl shift, which yields the *O*-centered radical **e8**. Conformational rearrangement *via* transition state **TS$_8$** converts **e8** to **z8** in the second step and generates a structure suitable for 1,4-[N↔O]-methyl shift. The last step, in which the *N*-centered radical **z5** is formed, is energetically the most demanding. The corresponding transition state **zTS$_{5/8}$** is 281.5 kJ mol^{-1} higher in energy than **e4**, but is still *ca.* 30 kJ mol^{-1} lower in energy (Table 3) than the rate-determining transition state **eTS$_{4/5}$** for the 1,2-[N↔O]-methyl shift described earlier (Scheme 2).

The experimentally observed EPR spectrum characterized through hyperfine coupling constants of a_N = 9.8 and a_H = 10.8 is in excellent agreement only with data calculated for radical **e4** with a_N = 9.6 and a_H = 10.9, in which the two oxygen atoms are in relative *trans*-position (Table 4). Radical **e4** can isomerize to its *cis*-form **z4**, but the latter is calculated 39.4 and 25.0 kJ mol^{-1} less stable in the gas phase (no explicit water included) and in aqueous solution, respectively (Table 3). As well, the calculated hfccs for the *cis*-isomer **z4** suggest that this structure does not contribute to the experimental splittings observed for the *N*-methylhydroxyurea radical (Table 4).

This journal is © The Royal Society of Chemistry 2012

Org. Biomol. Chem., 2012, **10**, 1196–1206 | 1199

Table 3 Relative energies (in kJ mol^{-1}, at 298.15 K) for structures involved in tautomerization, N,O-methyl shift, and conformational rearrangement processes of N-methylhydroxyurea-derived radicals $e4$ and $z4$

Name[a]	UBP86[b]	UB3LYP[b]	G3(MP2)RAD	G3B3	ΔG_{solv}[c]	G3B3 + ΔG_{solv}
$e4$	0.0	0.0	0.0	0.0	−50.1	0.0
$z4$	41.9	45.8	38.9	40.2	−67.7	22.6
$e5$	82.8	69.1	79.7	74.3	−61.4	63.0
$z5$	77.6	64.8	72.6	74.3	−47.9	76.5
$e6$	55.5	49.8	50.0	54.3	−38.9	65.5
$z6$	81.0	76.0	73.6	80.0	−54.3	75.8
$e7$	148.9	139.3	135.6	140.2	−54.2	136.1
$z7$	160.9	148.2	134.9	150.5	−59.5	141.1
$e8$	129.4	110.0	116.4	123.5	−49.3	124.3
$z8$	157.7	143.8	148.1	148.1	−61.9	136.3
TS$_4$	55.6	42.8	50.3	56.8	−56.1	50.8
TS$_5$	105.9	90.3	93.6	98.2	−48.7	99.6
TS$_6$	109.7	102.1	98.2	107.8	−51.5	106.4
TS$_7$	195.0	179.4	173.6	178.9	−63.9	165.1
TS$_8$	199.9	195.1	222.7	214.2	−52.8	211.5
eTS$_{4/5}$	298.6	303.3	300.4	306.9	−46.4	310.6
zTS$_{4/5}$	308.1	312.2	308.0	316.3	−52.6	313.8
eTS$_{4/6}$	64.5	76.7	85.4	91.0	−31.7	109.4
zTS$_{4/6}$	95.6	109.3	115.3	121.4	−50.7	120.8
eTS$_{5/7}$	142.2	154.0	159.4	164.5	−52.1	162.5
zTS$_{5/7}$	138.2	151.2	158.1	163.6	−52.2	161.5
eTS$_{4/8}$	229.8	251.7	292.4	278.9	−65.2	263.8
zTS$_{5/8}$	240.5	253.5	286.0	278.3	−46.9	281.5

[a] The most stable conformer considered. [b] 6-311++G(d,p) basis set employed. [c] Solvation energies calculated with CPCM/UAKS/UB3LYP/6-311+G(d,p) method in the model solvent (water) of $\varepsilon = 78.4$.
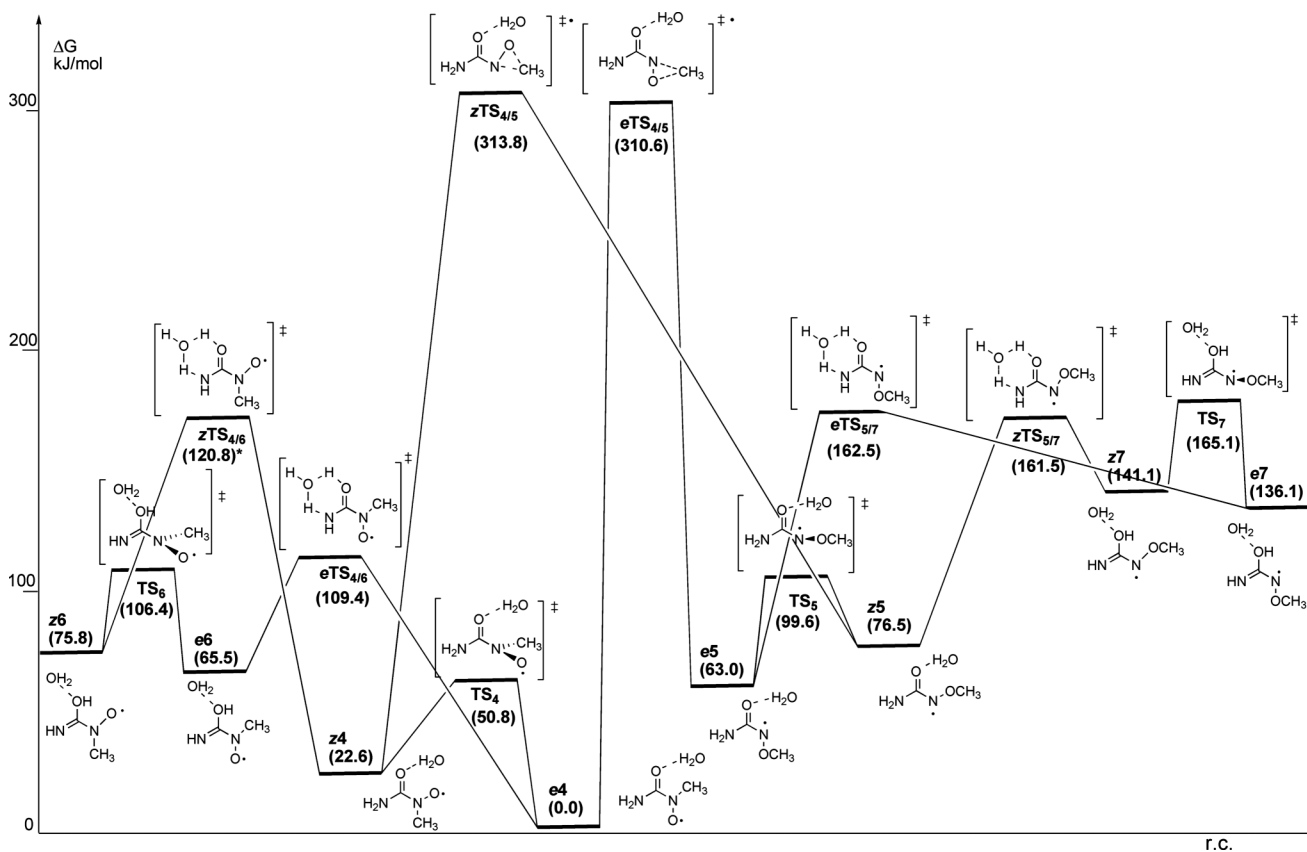
Scheme 2 Schematic energy profile (G3B3 + ΔG_{solv}) for tautomerization, 1,2-[N↔O]-methyl shift, and conformational processes in O-centered (**NMHU**, **4**) and N-centered (**OMHU**, **5**) monosolvated radicals. The energy of water-complexed radical **e4** is set to zero.
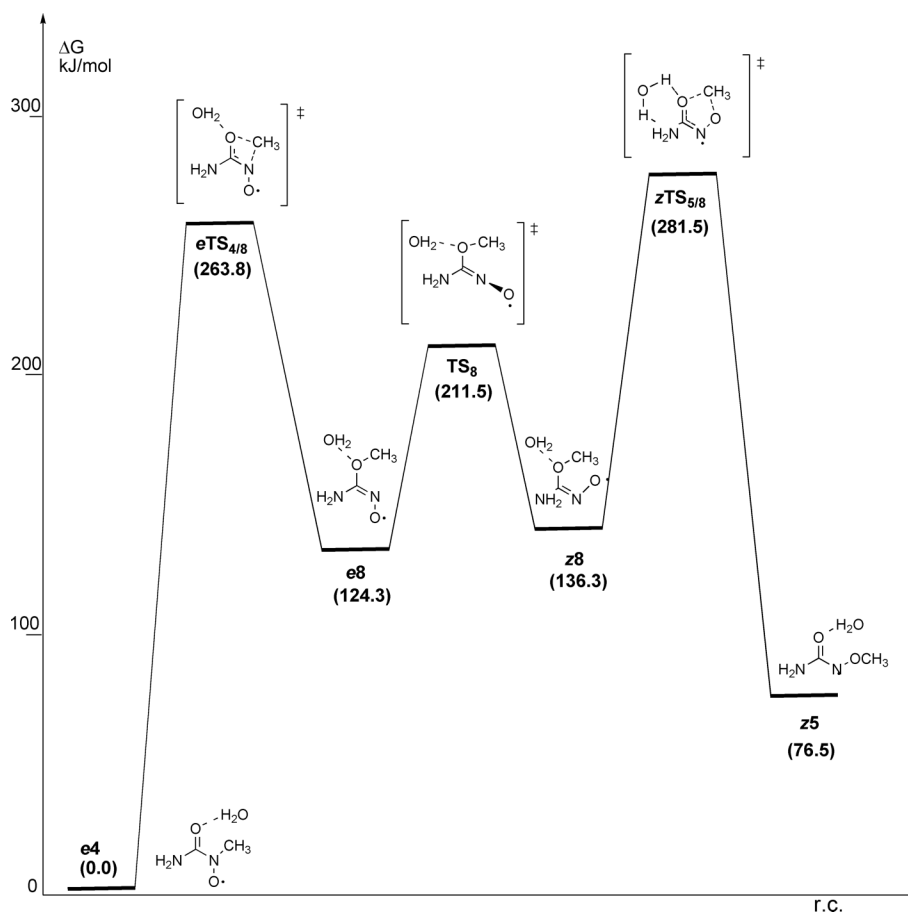
Scheme 3 Schematic energy profile (G3B3 + ΔG_{solv}) for 1,3-[N↔O]- and 1,4-[N↔O]-methyl shifts in *O*-centered monosolvated radicals *e4* and *z8*, respectively. The energy of water-complexed radical *e4* is set to zero.

Therefore, the hfcc calculations can be successfully used to distinguish between the two isomeric forms of *N*-methylhydroxyurea radical.

Spin density distribution values (Mulliken atomic spin densities, Fig. 2) in radical *e4* indicate that the spin is mainly located at the oxygen atom (0.519) with some contribution to the neighboring nitrogen (0.341), while the measured value of the g-factor (2.0068) is typical for oxygen-centered radical. This is represented by the singly occupied molecular orbital in *e4*, which is delocalized over the O atom and the adjacent N atom (Fig. 2). A similar spin distribution has been calculated ($SD_O = 0.551$, $SD_N = 0.365$) and a similar g-factor (2.0067) has been measured for the *O*-centered *N*-hydroxyurea radical in its *trans*-form *e1* (see above).

In addition to conformational changes, tautomerization processes in *O*-centered radicals *e4* and *z4* have also been considered (Scheme 2). Hydrogen atom migration from the –NH₂ group to carbonyl oxygen in *N*-methylhydroxyurea radicals was found to be a kinetically (the calculated rate constants $k_e = 4.2 \times 10^{-7}$ s^{-1} and $k_z = 4.8 \times 10^{-9}$ s^{-1}) and thermodynamically unviable process. The calculated energy barriers for reactions *e4* → *e6* and *z4* → *z6* are 109.4 and 120.8 kJ mol^{-1}, respectively. The iminolic forms *e6* and *z6* are 65.5 and 53.2 kJ mol^{-1} higher in energy than their amidic counterparts *e4* and *z4*, respectively (Table 3).
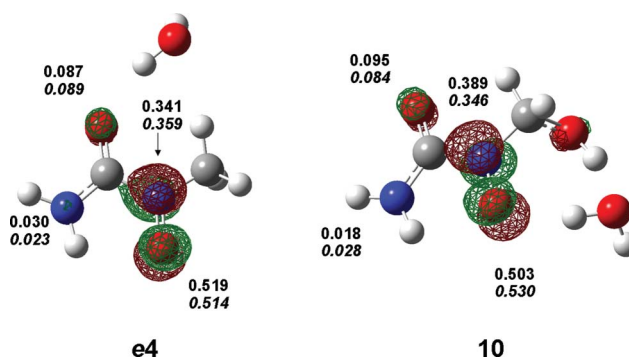

Fig. 2 UBP86/6-311++G(d,p) calculated SOMOs and spin distributions (Mulliken values) in water-complexed *N*-methylhydroxyurea-derived radicals *e4* (MO = 29) and **10** (MO = 33). Spin density values for gas-phase geometries (no explicit water is included) are in italics.

We have shown earlier[31] that the radical *e4* undergoes rearrangement in aqueous media. Unlike the oxidation of hydroxyurea with metal ions, in which only one radical has been detected, the oxidation of NMHU is characterized by consecutive formation of two different oxygen-centered free radicals, as recorded by EPR spectroscopy. The second paramagnetic species is represented by a seven resonance line EPR spectrum with different hyperfine

This journal is © The Royal Society of Chemistry 2012

Org. Biomol. Chem., 2012, **10**, 1196–1206 | 1201

Table 4 UB3LYP//UB3LYP/6-31G(d) calculated hfccs (a_{iso} in gauss)[a] for *N*-methylhydroxyurea-derived *O*-centered radicals

| Radical[b]	Isotropic hfccs	
	a_N	a_H
*e*4	9.2 (9.6)[c]	10.7 (10.9)
*z*4	8.6 (8.1)	9.6 (8.4)
*e*6	7.9 (8.7)	9.9 (10.4)
*z*6	21.1 (22.6)	8.0 (8.1)
*e*8	3.7 (4.6)	0.4 (0.3)
*z*8	3.6 (3.4)	1.1 (1.5)
Exp[d]	9.8	10.8
9	−3.1 (−3.6)	−10.9 (−11.9)
10	10.6 (9.1)	4.5 (4.7)
11	7.8 (8.9)	85.7 (94.7)
12	29.8	26.4/9.6[e]
Exp[d]	9.5	4.7

[a] The EPR-III basis set employed for C, H, and O atoms, and 6-31G(d) basis set for N atoms. [b] The most stable conformer considered. [c] Calculated hfccs for gas-phase geometries (no explicit water included) in parentheses. [d] Experimental values from ref. 31 [e] For H$_{cis}$ and H$_{trans}$, resp.

couplings suggesting a structural change in the vicinity of the unpaired electron. The *g*-factor of the rearranged radical is equal to that observed for *e*4, which is typical for oxygen-centered radicals. According to our experimental results, three different structures **9**, **10**, and **11** can be considered as possible products, along with the formaldoxime free radical **12** (Scheme 4). The latter radical can result from the oxidation of *N*-methylhydroxylamine radical, the hydrolysis product of the *e*4. The radical cation **9** has been suggested as a transient intermediate in the course of the *e*4 transformation process. The reaction of **9** with water results in the formation of **10**, which can subsequently rearrange to **11** *via* hydrogen migration. We have found that the only water-assisted pathway feasible for hydrogen migration is the process in which the water molecule is directly involved in forming seven-membered ring transition state (Scheme 4). The transition state structure **TS$_{10/11}$** has been located and calculated to be only 23.0 kJ mol^{-1} above **10**. As no direct spectroscopic evidence is available to rule out any of the candidates, quantum chemical calculations have been performed to interpret the resulting EPR parameters and to distinguish between the proposed structures.
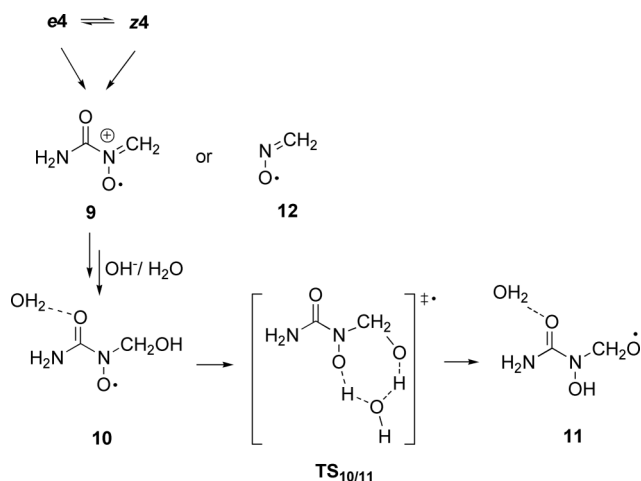
Scheme 4 Possible intermediates in rearrangements of *N*-methylhydroxyurea-derived radicals *e*4/*z*4.

The calculated hfccs clearly show that the free radical **10** is the most probable product, which is in agreement with conclusions based on preliminary experimental data.[31] Almost the same nitrogen hyperfine value (a$_N$ = 9.5 for **10** *vs*. a$_N$ = 9.8 for *e*4) in the two radicals indicates a similar spin density distribution (Scheme 5). The spin density in **10** is delocalized over the O (0.530) and N (0.346) atoms, which is represented by the SOMO that mostly includes these two atoms (Fig. 2). In the case of the two other proposed structures **9** and **11** very different spin distributions and isotropic hfccs are obtained computationally.
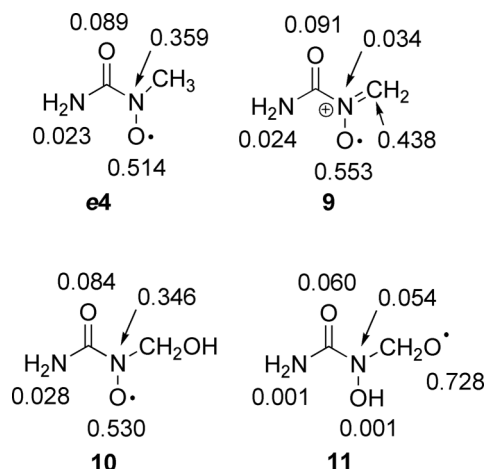
Scheme 5 UBP86/6-311++G(d,p) spin distributions (Mulliken values) in *O*-centered radical *e*4 and its rearranged products (for comparison reason, non-solvated species were considered only).

O-Methylhydroxyurea-derived radicals

An attempt to record a free radical generated from *O*-methylhydroxyurea in reaction with Fe(CN)$_6$$^{3-}$ by the EPR spectroscopy technique failed. The failure to detect the free radical derived from *O*-methylhydroxyurea indicates that this intermediate is present at much lower concentration than the free radicals generated either from hydroxyurea or *N*-methylhydroxyurea. This could be a consequence of a much lower stability of the former one (see Table 3), or due to its much slower formation (see below the conclusion on the O–H *vs*. N–H bond dissociation and radical stabilization energy values). In any case, the involvement of a free radical **5** in that reaction was assessed by initiating the polymerization of acrylamide.[30] The computational methods were applied to characterize structural properties of the radical **5** generated from *O*-methylhydroxyurea, and to compare its electronic properties to open-shell species generated from hydroxyurea or *N*-methylhydroxyurea.

It has been shown (see above) that the methyl shift reactions *e*4 → *e*5 or *z*4 → *z*5, which equilibrate *N*-centered and *O*-centered radicals, are energetically unfavorable processes (Δ*G*$^{#}$ > 300 kJ mol^{-1}). As well, the transition state structures *e*TS$_{5/7}$ and *z*TS$_{5/7}$ for tautomerization processes *e*5 → *e*7 and *z*7 → *z*7, respectively, are very high in energy (Table 3). Similar to the case of *N*-methylhydroxyurea-derived radicals, the iminolic tautomers of *O*-methylhydroxyurea-derived radicals *e*7/*z*7 are significantly higher in energy than the corresponding amidic tautomers *e*5/*z*5. Thus, the only feasible rearrangement (the calculated rate constant

1202 | *Org. Biomol. Chem.*, 2012, **10**, 1196–1206

This journal is © The Royal Society of Chemistry 2012

$k = 2.4 \times 10^6$ s^{-1}) of radical $e5$ is conformational isomerization to $z5$ for which the calculated energy barrier is 36.6 kJ mol^{-1}. The *trans* configured radical $e5$ is more stable than *cis* form $z5$ (Table 3), which is similar to the cases of HU and NMHU.

Atomic spin densities in *trans*-form $e5$ indicate (Fig. 3) that the spin is mainly located at the nitrogen atom (0.636) with some contribution to the neighboring O atom (0.225), but also to the carbonyl oxygen atom (0.134). In *cis*-form $z5$ the participation of the neighboring oxygen in spin delocalization is somewhat larger (0.263), while the contribution of carbonyl oxygen atom is negligible (0.065).
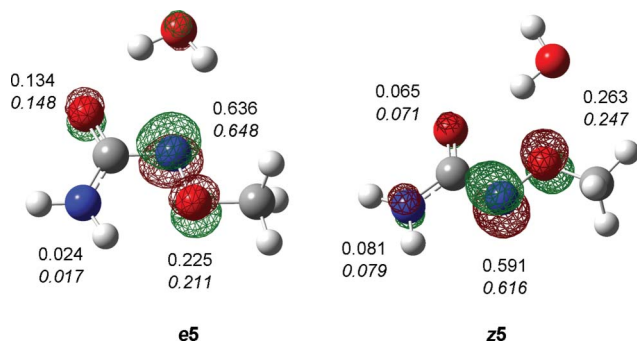

Fig. 3 UBP86/6-311++G(d,p) calculated SOMOs and spin distributions (Mulliken values) in water-complexed *O*-methylhydroxyurea-derived radicals $e5$ and $z5$. Spin density values for gas-phase geometries (no explicit water is included) are in italics.

The calculated hfccs values for $e5$ ($a_N = 2.8$ and $a_H = 5.1$) and $z5$ ($a_N = 2.8$ and $a_H = 5.8$) are very similar, suggesting that EPR studies cannot be used as a decisive probe for the identification of the preferred isomer in the equilibrium. This is contrary to the case of the *O*-centered radical **4**, where the hfcc calculations can be successfully used to distinguish between the two isomeric *cis/trans* forms (see above).

Reduction potential of hydroxyureas

It has been shown that NMHU is more reactive than HU towards oxyhemoglobin. Similarly, a higher reactivity of the free radical derived from NHMU than the corresponding radical derived from HU towards metal ions has been measured. OMHU does not react with hemoglobin, but slow oxidation with hexacyanoferrate ions has been observed. In order to compare differences in the redox behaviour of HU and its methylated analogues, NMHU and OMHU, the reduction potential for each anion/radical pair has been calculated at the G3B3 level of theory. The dependence of the rate of oxidation of hydroxyureas on the acidity of aqueous solution shows that the anions are much more reactive than the corresponding molecular forms.[30,36] Therefore, only the respective water-complexed anions **13**, **14**, and **15** (Fig. 4) have been considered as redox active species for the calculation of reduction potentials.

The question concerning the actual site of ionization (protonation and deprotonation) of hydroxyureas and hydroxamic acids has been long debated.[45–50] In the course of our investigation of hydroxamic acid properties, we have reported potentiometric and computational results for thermodynamic parameters
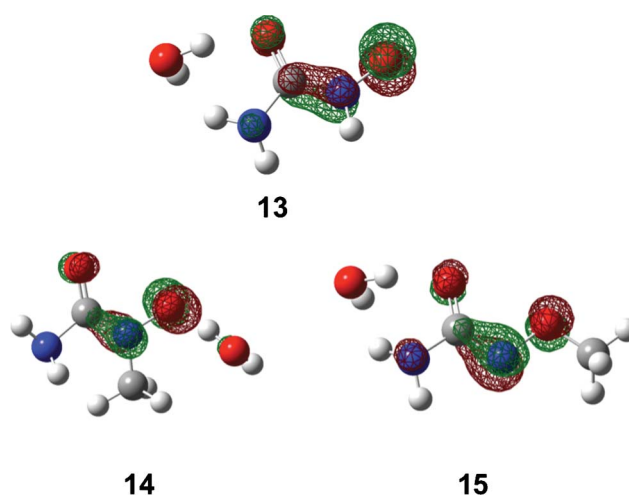

Fig. 4 BP86/6-311++G(d,p) calculated HOMOs in water-complexed anions derived from hydroxyurea (**13**; MO = 25, isoval = 0.08), *N*-methylhydroxyurea (**14**; MO = 29), and *O*-methylhydroxyurea (**15**; MO = 29).

of ionization for hydroxyurea, *N*-methylhydroxyurea, and *O*-methylhydroxyurea.

The results indicate that both HU and NMHU behave as *O*-acids, *i.e.* the deprotonation occurs at the hydroxamate oxygen atom, whereas the dominant deprotonation site in OMHU is the hydroxamate nitrogen atom.[30,51,52] The most stable monosolvated oxyanions **13** and **14** of HU and NMHU, respectively, and *N*-deprotonated anionic form **15** derived from OMHU are presented in Fig. 4. The calculated HOMO of oxyanions **13** and **14**, from which the electron transfer to hemoglobin or metal ion oxidant is expected to occur,[53] is composed mostly of the hydroxamate oxygen p atomic orbital, with significant contribution from the hydroxamate nitrogen p AO, while the participation of the carbonyl oxygen atom in the HOMO is negligible (Fig. 4). In the case of *O*-methylhydroxyureate **15**, the calculated HOMO is mostly located on the hydroxamate nitrogen with some contribution from carbonyl oxygen and neighbouring oxygen atom.

Absolute reduction free energy in aqueous solution can be calculated (thermodynamic cycles used in the computation of equilibrium reduction potentials are presented in the ESI†) routinely by computing the energy components of the reduced (anionic form) and oxidized (free radical) species. Thus, ΔG^{EA}_{aq} is defined by the following equation:

$$\Delta G^{EA}_{aq} = G^0_g \text{ (red)} + \Delta G^0_{solv} \text{ (red)} - [G^0_g \text{ (ox)} + \Delta G^0_{solv} \text{ (ox)}] \quad (1)$$

Solvation free energies, ΔG^0_{solv}, were evaluated by a SCRF approach based on the CPCM model at the B3LYP/6-311+G(d,p) level. Reduction potentials, E^0, relative to the standard hydrogen electrode (SHE) were evaluated from the electron affinities in aqueous solution, ΔG^{EA}_{aq}, obtained from the G3B3 calculations for hydroxyureas **13**, **14**, and **15** and the respective radicals $z1$, $z4$, and $z5$, according to:

$$E^0 = - \Delta G^{EA}_{aq}/nF + E^0_{SHE} \quad (2)$$

where n is the number of electrons, F is the Faraday constant (96 485 J K^{-1} mol^{-1}), and E^0_{SHE} is the absolute reduction potential of the SHE ($E^0_{SHE} = -4.36$ V),[55] *cf.* the protocol of Truhlar and coworkers.[56]

Table 5 Reduction free energies (ΔG^{EA}_{aq} in kJ, at 298.15 K) and calculated standard reduction potentials (E^0 in V, at 298.15 K) for anion/radical pairs of hydroxyurea and its methylated analogues in water[a]

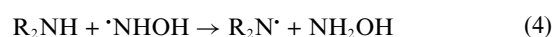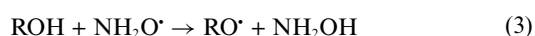|	Redox couple radical/anion	ΔG^{EA}_{aq}	E^0	E^0_{exp}
HU	**z1/13**	−396.6	+0.25	+0.47[b];
		(−387.1)[d]	(+0.35)	+0.73[c]
NMHU	**z4/14**	−401.1	+0.20	—
		(−345.9)	(+0.77)	
OMHU	**z5/15**	−430.8	−0.11	—
		(−438.9)	(−0.19)	

[a] All calculations were performed at G3B3 level and solvation effects were included by CPCM-B3LYP/6-311+g(d,p) model. [b] Experimental value[16d] has been estimated from kinetic measurements. [c] Experimental value[54] has been estimated from cyclic voltammetry measurement. [d] Calculated ΔG^{EA}_{aq} and E^0 for gas-phase geometries (no explicit water included) are in parentheses.

The data for the reduction potential of the free radical/anion couples relevant for this study are collected in Table 5. From the calculated data for non-solvated species one can conclude that the most reactive anion is **14**, *i.e.* its reduction potential is the most positive (+0.77). This is in agreement with experimental findings which reveal that *N*-methylhydroxyurea reacts with hemoglobin and metal ions faster than the parent hydroxyurea.[21,30] The calculated reduction potential of the hydroxyurea anion **13** is similar to the experimental value estimated from kinetic measurements, but differs from the value determined by cyclic voltammetry.[57] The use of one explicit water molecule reduces the reduction potential for hydroxyurea and *N*-methylhydroxyurea, with the former having slightly more positive E^0 value. It is possible that additional water molecules should be considered explicitly in order to reproduce the experimental trend observed for hydroxyurea and *N*-methylhydroxyurea. It has been shown recently that differential solvation effects on the anion and neutral radical can strongly influence the thermodynamics of one-electron reduction, *i.e.* the agreement between calculated and experimental reduction potential in the model solvent is typically poorer.[58] Finally, the reduction potential for *O*-methylhdroxyureate **15** is the lowest one, *i.e.* negative value is calculated in the case of non-solvated and monosolvated species, which in part explains our unsuccessful attempt to detect the corresponding radical **e5/z5** by EPR spectrometry.

Radical stability — RSE and BDE values

In order to compare the stabilities and reactivities for the two different subclasses of hydroxyurea-derived radicals (*O*- and *N*-centered), radical stabilization energies (RSE) were calculated and bond dissociation energies (BDE) were estimated for energetically relevant species (**1**, **2**, **4**, and **5**) and compared to biologically important radicals (amino, aminoxyl, phenoxy, *para*-methylphenoxy, hydroxyl).

RSE have been calculated as the reaction enthalpies at 298.15 in the gas-phase (with no explicit water molecule) for isodesmic H-transfer reactions 3 and 4:[28,59]

$$\text{ROH} + \text{NH}_2\text{O}^\bullet \rightarrow \text{RO}^\bullet + \text{NH}_2\text{OH} \qquad (3)$$

$$\text{R}_2\text{NH} + {}^\bullet\text{NHOH} \rightarrow \text{R}_2\text{N}^\bullet + \text{NH}_2\text{OH} \qquad (4)$$
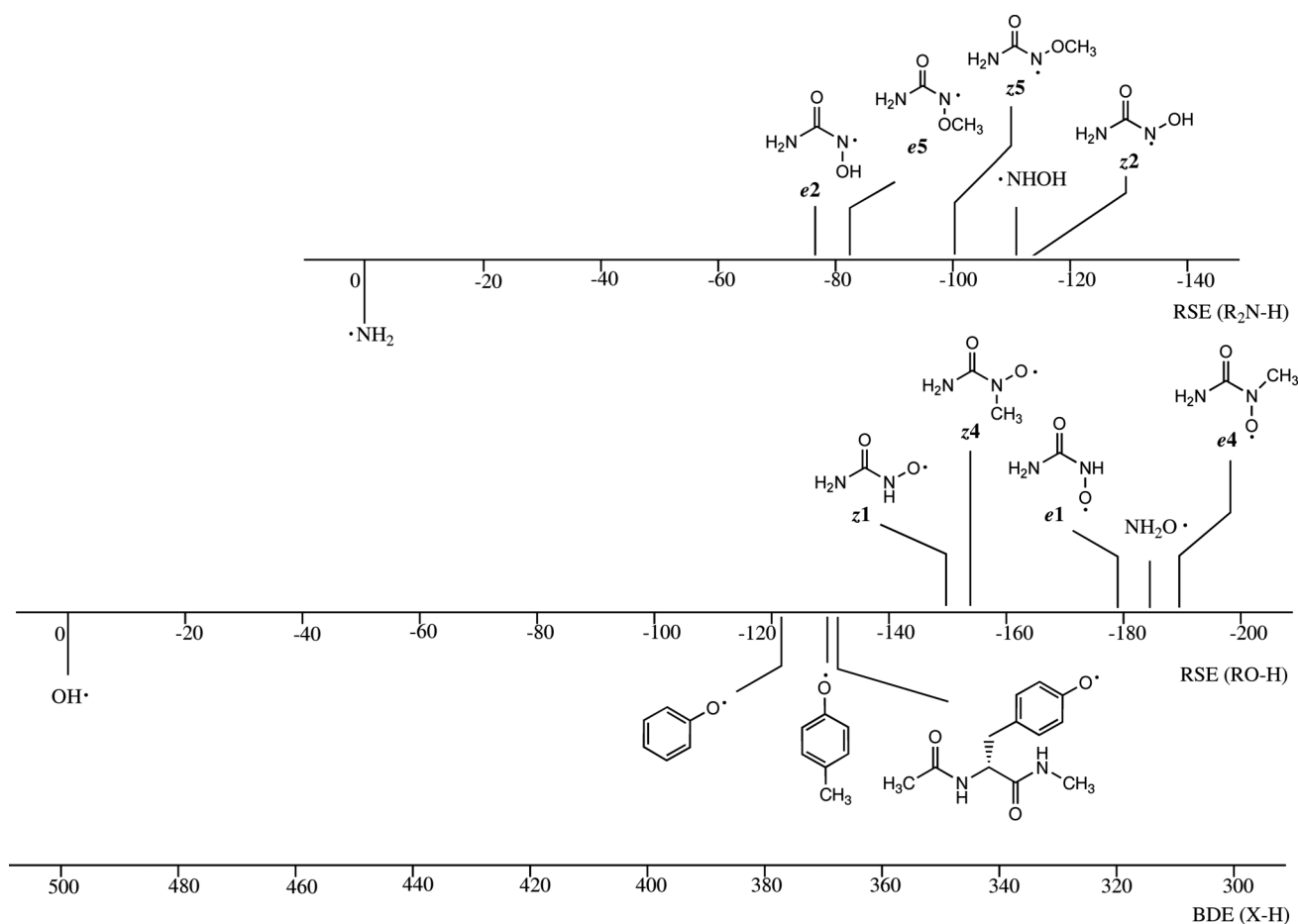
where R are substituents as presented in Scheme 6. These RSE values can be understood as the influence of the substituent on the homolytic BDE of the respective reference molecules (negative values imply a stabilizing effect of the substituent). The thermodynamic stabilities of the *O*- and *N*-centered radicals have been referenced to that of aminoxyl radical $\text{NH}_2\text{O}^\bullet$ or its isomeric form ${}^\bullet\text{NHOH}$, respectively.

The RSE values have been combined with the experimentally determined X–H BDE in hydroxylamine with the N–H BDE = 341 ± 2 kJ mol⁻¹ and the O–H BDE = 318 ± 4 kJ mol⁻¹.[60] In addition, the zero-point of the stability scale of *O*-centered radicals is located at 497.1 kJ mol⁻¹ (due to O–H BDE in water), while the zero-point of the scale for *N*-centered radicals is shifted by 47 kJ mol⁻¹ (due to lower N–H BDE value in the reference compound NH₃; 450.1 kJ mol⁻¹). This type of presentation allows for a comparison of the stabilities of radicals characterized through different reference systems (HO• and •NH₂), the direct correspondence of RSE and BDE values becomes visible, and exothermic radical transformations involving hydrogen transfer reactions are easily recognized.

According to the estimated BDE values (Scheme 6), *O*-centered radicals **e1** and **e4** derived from hydroxyurea and *N*-methylhydroxyurea, respectively, are the most stable open-shell species. The homolytic cleavage of the bonds leading to these radicals requires similar thermochemical effort with O–H BDE (**e1**) = 317.9 kJ mol⁻¹ and O–H BDE (**e4**) = 308.4 kJ mol⁻¹, while the corresponding BDE values for phenoxy, *para*-methylphenoxy, and tyrosyl dipeptide radicals (Scheme 6) are *ca.* 360, 363, and 365 kJ mol⁻¹, respectively.[61] The latter compounds are related to tyrosyl radicals, which are relevant for biological activity of hydroxyurea and its methylated analogues.[23,24] Due to the difference in the respective BDE values, one can predict that hydrogen atom transfers from HU and NMHU to the tyrosyl radical (as expected in the tyrosyl radical quenching mechanism) are thermochemically favorable processes, with NMHU being more exothermic by *ca.* 10 kJ mol⁻¹. These results also imply that OMHU (N–H BDE (**e5**) = 368 kJ mol⁻¹) is less likely to be an effective reducing agent for phenoxy type-radicals, as shown earlier by experimental studies.

Computational Details

Restricted and unrestricted DFT calculations are employed for geometry optimizations and frequency calculations for closed- and open-shell systems, respectively. B3LYP/6-311++G(d,p) and BP86/6-311++G(d,p) methods are used. All energies are reported at 298.15 K. Improved thermodynamic energetics have been calculated with G3B3[62] and G3(MP2)-RAD[63] composite models. The latter method, which is quite cost-effective and gives essentially the same results as G3B3, has recently been optimized for open-shell systems.[64] The (U)CCSD(T)/6-31G(d) calculations for the G3(MP2)-RAD model have been performed with MOLPRO 2006.1,[65] while all other calculations have been performed with Gaussian 09.[66] Solvation free energies have been determined using the conductor-like polarizable continuum model (CPCM) on B3LYP/6-311+G(d,p) level, with UAKS atom radii definition and electrostatic scaling factor (alpha value) set to 1.2 for all atoms. The most stable forms of water-complexed (monosolvated)

1204 | *Org. Biomol. Chem.*, 2012, **10**, 1196–1206

This journal is © The Royal Society of Chemistry 2012

Scheme 6 Radical stabilization energies (RSE) of selected *O*- and *N*-centered radicals and bond dissociation energies (BDE) of the corresponding O–H and N–H bonds. All calculated values are obtained at the G3B3 level.

species are located by placing a water molecule in a variety of locations to sample the different arrays of interaction networks available between the corresponding radical/anion and water. Initial configurations were created using a locally modified version of the stochastic search method.[30,67] Hyperfine coupling constants (hfccs) were calculated using the EPR-III basis set for C-, H-, O- atoms, while 6-31G(d) was used for nitrogen atoms, according to the procedure reported earlier.[38] Natural population analysis (NPA) was done using NBO 3.1 program,[68] as included in the Gaussian program package.

Acknowledgements

Notes and references

1 J. L. Spivak and H. Hasselbalch, *Expert Rev. Anti-Infect. Ther.*, 2011, **11**, 403.
2 S. Hannessian and S. Johnstone, *J. Org. Chem.*, 1999, **64**, 5896.
3 P. Nandy, E. J. Lien and V. I. Avramis, *Anticancer Res.*, 1999, **19**, 1625.
4 A. Kleeman, J. Engel, B. Kutscher and D. Reichert, *Pharmaceutical substances, synthesis, patents, applications*, 4th edn Thieme, Stuttgart, 2001.
5 S. B. King, *Free Radical Biol. Med.*, 2004, **37**, 737.
6 N. Saban and M. Bujak, *Cancer Chemother. Pharmacol.*, 2009, **64**, 213.
7 H. S. Rosenkranz, E. B. Winshell, A. Mednis, H. S. Carr and C. J. Ellner, *J. Bacteriol.*, 1967, **94**, 1025.
8 N. K. Sinha and D. P. Snustad, *J. Bacteriol.*, 1972, **112**, 1321.
9 J. A. Fuchs and H. O. Karlstrom, *Eur. J. Biochem.*, 1973, **32**, 457.
10 B. Kren and J. A. Fuchs, *J. Bacteriol.*, 1987, **169**, 14.
11 B. M. Sjoberg, S. Hahne, M. Karlsson, H. Jornvall, M. Goransson and B. E. Uhlin, *J. Biol. Chem.*, 1986, **261**, 5658.
12 J. L. Sneeden and L. A. Loeb, *J. Biol. Chem.*, 2004, **279**, 40723.
13 T. Bollenbach and R. Kishony, *Mol. Cell*, 2009, **36**, 728.
14 B. W. Davies, M. A. Kohanski, L. A. Simmons, J. A. Winkler, J. J. Collins and G. C. Walker, *Mol. Cell*, 2009, **36**, 845.
15 S. Charache, M. L. Terrin, R. D. Moore, G. J. Dover, F. B. Barton, S. V. Eckert, R. P. McMahon and D. R. Bonds, *N. Engl. J. Med.*, 1995, **332**, 1317.
16 E. Boyland and R. Nery, *J. Chem. Soc. C*, 1966, 354; A. R. Forrester, M. M. Ogilvy and R. H. Thomson, *J. Chem. Soc. C*, 1970, 1081; A. Budimir, E. Bešić and M. Biruš, *Croat. Chem. Acta*, 2009, **82**, 807; E. E. Smissuan, N. A. Dahle and V. D. Warner, *J. Org. Chem.*, 1971, **38**, 2565; D. Chatterjee, K. A. Nayak, E. Ember and R. van Eldik, *Dalton Trans.*, 2010, **39**, 1695.
17 H. Bartsch, J. A. Miller and E. C. Miller, *Biochim. Biophys. Acta, Gen. Subj.*, 1972, **273**, 40; J. M. Huang, E. M. Sommers, D. B. Kim-Shapiro and S. B. King, *J. Am. Chem. Soc.*, 2002, **124**, 3473.

18 R. Pacelli, J. Taira, J. A. Cook, D. A. Wink and M. C. Krishna, *Lancet*, 1996, **347**, 900; Y. Samuni, W. Flores-Santana, M. C. Krishna, J. B. Mitchell and D. Wink, *Free Radical Biol. Med.*, 2009, **47**, 419; C. L. Ritter, D. Malejkagiganti and C. F. Polnaszek, *Chem.-Biol. Interact.*, 1983, **46**, 317; K. Sato, T. Akaike, T. Sawa, Y. Miyamoto, M. Suga, M. Ando and H. Maeda, *Cancer Sci.*, 1997, **88**, 1199.

19 S. B. King, *Curr. Med. Chem.*, 2003, **10**, 437.

20 K. Sakano, S. Oikawa, K. Hasegawa and S. Kawanishi, *Cancer Sci.*, 2001, **92**, 1166; C. D. Mull, C. L. Bonifant, G. Yasaki, E. C. Palmer, H. Shields, S. K. Ballas, D. B. Kim-Shapiro and S. B. King, *J. Org. Chem.*, 1998, **63**, 6452.

21 J. Huang, Z. Zou, D. B. Kim-Shapiro, S. K. Ballas and S. B. King, *J. Med. Chem.*, 2003, **46**, 3748.

22 B. Rohrman and D. A. Mazziotti, *J. Phys. Chem. B*, 2005, **109**, 13392.

23 J. Fritscher, E. Artin, S. Wnuk, G. Bar, J. H. Robblee, S. Kacprzak, M. Kaupp, R. G. Griffin, M. Bennati and J. Stubbe, *J. Am. Chem. Soc.*, 2005, **127**, 7729.

24 H. Zipse, E. Artin, S. Wnuk, G. J. S. Lohman, D. Martino, R. G. Griffin, S. Kacprzak, M. Kaupp, B. Hoffman, M. Bennati, J. Stubbe and N. Lees, *J. Am. Chem. Soc.*, 2009, **131**, 200.

25 W. Jiang, J. Xie, P. Varano, C. Krebs and J. M. Jr. Bollinger, *Biochemistry*, 2010, **49**, 5340.

26 G. X. Chen and K. Asada, *J. Biol. Chem.*, 1990, **265**, 2775.

27 K. Kawamoto, G.-X. Chen, J. Mano and K. Asada, *Biochemistry*, 1994, **33**, 10487.

28 H. Zipse, *Top. Curr. Chem.*, 2006, **263**, 163.

29 J. Hioe and H. Zipse, *Org. Biomol. Chem.*, 2010, **8**, 3609.

30 A. Budimir, T. Weitner, I. Kos, D. Šakić, M. Gabričević, E. Bešić and M. Biruš, *Croat. Chem. Acta*, 2011, **84**, 133.

31 T. Weitner, E. Bešić, I. Kos, M. Gabričević and M. Biruš, *Tetrahedron Lett.*, 2007, **48**, 9021.

32 In the case of *e1* the unpaired electron is in A″ orbital (^{2}A″ electronic state with Cs symmetry). The corresponding ^{2}A′ electronic state is calculated 172.7 kJ mol^{-1} less stable than the ^{2}A″ state.

33 Similar has been observed for the *trans*- and *cis*-forms of hydroxyurea anions, see: M. Remko, P. D. Lyne and W. G. Richards, *Phys. Chem. Chem. Phys.*, 1999, **1**, 5353.

34 V. Vrček and H. Zipse, *J. Org. Chem.*, 2009, **74**, 2947.

35 G. Lassmann and B. Liermann, *Free Radical Biol. Med.*, 1989, **6**, 241.

36 M. Gabričević, E. Bešić, M. Biruš, A. Zahl and R. van Eldik, *J. Inorg. Biochem.*, 2006, **100**, 1606.

37 N. Rega, M. Cossi and V. Barone, *J. Chem. Phys.*, 1996, **105**, 11060.

38 L. Hermosilla, P. Calle, J. M. Garcia de la Vega and C. Sieiro, *J. Phys. Chem. A*, 2006, **110**, 13600; L. Hermosilla, J. M. Garcia de la Vega, C. Sieiro and P. Calle, *J. Chem. Theory Comput.*, 2011, **7**, 169.

39 I. Komaromi and J. M. J. Tronchet, *THEOCHEM*, 1997, **401**, 55.

40 H. M. Muchall, N. H. Werstiuk and J. Lessard, *THEOCHEM*, 1999, **469**, 135 .

41 S. Simon, M. Sodupe and J. Bertran, *Theor. Chem. Acc.*, 2004, **111**, 217; L. Rodriguez-Santiago, O. Vendrell, I. Tejero, M. Sodupe and J. Bertran, *Chem. Phys. Lett.*, 2001, **334**, 112; J. W. Gauld, H. Audier, J. Fossey and L. Radom, *J. Am. Chem. Soc.*, 1996, **118**, 6299.

42 The atomic spin density on carbon atoms in **1** and **2** is negligible (all calculated values are less than 0.009), whereas in **3** the corresponding spin density is larger than 0.160.

43 Tautomerizations of radicals *e1* or *z1* in which the H atom is transferred from an amino group to a carbonyl oxygen result in intermediates which are very unstable (see ESI†).

44 J. Huang, S. B. Hadimani, J. W. Rupon, S. K. Ballas, D. B. Kim-Shapiro and S. B. King, *Biochemistry*, 2002, **41**, 2466.

45 A. Bagno, C. Comuzzi and G. Scorrano, *J. Am. Chem. Soc.*, 1994, **116**, 916.

46 A. Bagno and C. Comuzzi, *Eur. J. Org. Chem.*, 1999, **1**, 287.

47 M. Remko, P. D. Lyne and W. G. Richards, *Phys. Chem. Chem. Phys.*, 2000, **2**, 2511.

48 M. Remko and C.-W. von Lieth, *Struct. Chem.*, 2004, **15**, 285.

49 G. Di Gregorio, G. La Mamna, J. C. Paniagua and E. Vilaseca, *THEOCHEM*, 2000, **673**, 87.

50 B. Monzyk and A. L. Crumbliss, *J. Org. Chem.*, 1980, **45**, 4670.

51 I. Vinković Vrček, I. Kos, T. Weitner and M. Biruš, *J. Phys. Chem. A*, 2008, **112**, 11756.

52 I. Vinković Vrček, *Ph. D. Thesis*, University of Zagreb, Zagreb, 2007.

53 If inner-shell electron transfer is assumed, *z*-forms of anions are to be considered only. See ref. 30,51, and 52.

54 K.-Y. Lam, D. G. Fortier and A. G. Sykes, *J. Chem. Soc., Chem. Commun.*, 1990, 1019.

55 A. Lewis, J. A. Bumpus, D. G. Truhlar and C. J. Cramer, *J. Chem. Educ.*, 2004, **81**, 596.

56 P. Winget, C. J. Cramer and D. G. Truhlar, *Theor. Chem. Acc.*, 2004, **112**, 217.

57 It is likely that the reduction potential for hydroxyurea estimated from cyclic voltametry is not related to one-, but to two-electron transfer processes.

58 D. I. Pattison, R. J. O'Reilly, O. Skaff, L. Radom, R. F. Anderson and M. J. Davies, *Chem. Res. Toxicol.*, 2011, **24**, 371.

59 J. Hioe and H. Zipse, *Faraday Discuss.*, 2010, **145**, 301.

60 D. A. Dixon, J. S. Francisco and Y. Alexeev, *J. Phys. Chem. A*, 2006, **110**, 185; J. Lind and G. Merenyi, *J. Phys. Chem. A*, 2006, **110**, 192.

61 J. Hioe, G. Savasci, H. Brand and H. Zipse, *Chem.–Eur. J.*, 2011, **17**, 3781.

62 A. G. Baboul, L. A. Curtiss, P. C. Redfern and K. Raghavachari, *J. Chem. Phys.*, 1999, **110**, 7650.

63 L. A. Curtiss, K. Raghavachari, P. C. Redfern, V. Rassolov and J. A. Pople, *J. Chem. Phys.*, 1998, **109**, 7764; D. J. Henry, M. B. Sullivan and L. Radom, *J. Chem. Phys.*, 2003, **118**, 4849.

64 D. J. Henry, C. J. Parkinson and L. Radom, *J. Phys. Chem. A*, 2002, **106**, 7927.

65 MOLPRO, version 2006.1, a package of *ab initio* programs written by H.-J. Werner, P. J. Knowles, G. Knizia, F. R. Manby, M. Schütz, P. Celani, T. Korona, R. Lindh, A. Mitrushenkov, G. Rauhut, K. R. Shamasundar, T. B. Adler, R. D. Amos, A. Bernhardsson, A. Berning, D. L. Cooper, M. J. O. Deegan, A. J. Dobbyn, F. Eckert, E. Goll, C. Hampel, A. Hesselmann, G. Hetzer, T. Hrenar, G. Jansen, C. Köppl, Y. Liu, A. W. Lloyd, R. A. Mata, A. J. May, S. J. McNicholas, W. Meyer, M. E. Mura, A. Nicklaß, D. P. O'Neill, P. Palmieri, K. Pflüger, R. Pitzer, M. Reiher, T. Shiozaki, H. Stoll, A. J. Stone, R. Tarroni, T. Thorsteinsson, M. Wang, A. Wolf; see http://www.molpro.net.

66 *Gaussian 09, Revision A.1*, M. J. Frisch, G. W. Trucks, H. B. Schlegel, G. E. Scuseria, M. A. Robb, J. R. Cheeseman, G. Scalmani, V. Barone, B. Mennucci, G. A. Petersson, H. Nakatsuji, M. Caricato, X. Li, H. P. Hratchian, A. F. Izmaylov, J. Bloino, G. Zheng, J. L. Sonnenberg, M. Hada, M. Ehara, K. Toyota, R. Fukuda, J. Hasegawa, M. Ishida, T. Nakajima, Y. Honda, O. Kitao, H. Nakai, T. Vreven, J. A. Montgomery, Jr., J. E. Peralta, F. Ogliaro, M. Bearpark, J. J. Heyd, E. Brothers, K. N. Kudin, V. N. Staroverov, R. Kobayashi, J. Normand, K. Raghavachari, A. Rendell, J. C. Burant, S. S. Iyengar, J. Tomasi, M. Cossi, N. Rega, J. M. Millam, M. Klene, J. E. Knox, J. B. Cross, V. Bakken, C. Adamo, J. Jaramillo, R. Gomperts, R. E. Stratmann, O. Yazyev, A. J. Austin, R. Cammi, C. Pomelli, J. W. Ochterski, R. L. Martin, K. Morokuma, V. G. Zakrzewski, G. A. Voth, P. Salvador, J. J. Dannenberg, S. Dapprich, A. D. Daniels, Ö. Farkas, J. B. Foresman, J. V. Ortiz, J. Cioslowski, and D. J. Fox, Gaussian, Inc., Wallingford CT, 2009.

67 M. Saunders, *J. Comput. Chem.*, 2004, **25**, 621; V. Vrček, O. Kronja and M. Saunders, *J. Chem. Theory Comput.*, 2007, **3**, 1223; M. A. Addicoat and G. F. Metha, *J. Comput. Chem.*, 2009, **30**, 57.

68 NBO Version 3.1, E. D. Glendening, A. E. Reed, J. E Carpenter, F. Weinhold.